CHARACTERIZATION AND EVALUATION ON HUMIDITY BASED PROTON CONDUCTIVITY OF LEAD-L-TARTRATE COORDINATION COMPOUND

G.Bhuvaneswari[a], P.Palani Murugan[a], C.Nirmala[b],K.Velumani[a], M.Obulichetty[c], S.S.Subramanian[b], S.Annapoorani[d], S.Rameshkumar[a]*

a. Department of Chemistry, Sri Vasavi College, Erode, Tamilnadu, India – 638316.
b. Akshaya college of Engineering and Technology, Kinathukadavu, Tamilndu,India-642109.
c. Department of Applied Science, PSG College of Technology, Coimbatore, India-641004.
d. Deapartment of Chemistry, LRG Government Arts College for Women, Tirupur, India-641604.
*Mail ID of Corresponding Author: srksvc2016@gmail.com

Abstract: The low proton conductivity of proton-conducting solids at reduced relative humidity (RH) hinders the performance of fuel cells. Even though various proton conducting frameworks have been developed, the conductivity of such methods dropped due to weak host–guest interactions of complex synthesis process, posing significant damage in increasing temperatures, limited practical use owing to the high costs. Therefore, the development of new and inexpensive proton-conducting materials with excellent performance has been the subject of intensive research. Hence, in this paper, an environmentally benign coordination polymer called Manganese-based proton conducting material that possesses the structural architectures as those of the other proton conducting metal-organic framework (MOF) and Coordination Polymers (CP) is presented. In order to aid the electrochemical characteristics of the compound, the method involves a crystallization process simply by plain mixing of inexpensive aqueous precursors. The relationship between structural characteristics and the nature of proton conductivity has been explored. The Fourier transform infrared spectroscopy (FT-IR) and Powder X-ray diffraction (PXRD) analysis are carried out to investigate the structural stability of the model under varying atmospheric conditions. Relative to other MOFs, the presented work has a high proton conductivity of 8.4×10^{-4} S cm^{-1} at 98% RH as compared to the existing methods. These results signify the crucial role of the water vapor and the protic molecules in the creation of H^+ charges and the hydrogen-bonded pathways in the system.

Key Words: *Manganese, Metal-Organic Frameworks (MOF), Coordination Polymers (CP), Proton Conductivity, Hydrogen-Bonded Networks, Solid electrolytes*

1. INTRODUCTION

In the fields of energy and material chemistry, the design and preparation of proton conducting materials has been a hot topic due to their clean energy features of high energy conversion rate and near-zero emission, and so on. The first proton conductive material utilized in practical fuel cell applications was Nafion, a perfluorinated sulfonated polymer, discovered in the late 1960s (Lee et al., 2020). Nafion was found effective as a membrane for proton-conducting fuel cells by permitting hydrogen ion transport while preventing electron conduction (Guccini et al., 2019). The structure of the Nafion membrane consists of the cluster channel that is labelled as the first unit for its component. The 4-nm structure of the Nafion is linked together with the water structure that has a diameter of 1 nm that is equally discrete within the hydrophobic backbones (Sazali et al., 2020). Although the conventional Nafions show high performance with H_2O conducting medium, the high price of the material and the efficiency degradation during the cyclic hydration and dehydration processes are the drawbacks. Therefore, the development of alternative materials is required (Lim & Kitagawa, 2021).

In the past three decades, crystalline porous materials, such as coordination polymers (CPs) and Metal-Organic Frameworks (MOFs) have been proven as promising candidates in the field of energy conversion applications, heterogeneous catalysis, gas storage, selective sensing and separations

of small molecules and ionic conductivities(Biradha et al., 2021). In particular, the tuneability and functionality of CPs and MOFs provide an opportunity to replace conventional materials. More importantly, abundant oxygen atoms from interchain NO_3^- anions and lattice H_2O molecules generate hydrogen bond networks throughout the whole crystal, which are perfect proton transport channels for humidity sensing (T. Li et al., 2019).As a result, a fundamental understanding of molecular motion in the conducting media helps to anticipate the overall conduction mechanism in MOFs (Kolokolov et al., 2020).

The crystalline nature of MOFs enables interrogation of the mechanisms of proton conduction, thus providing key insights into the design of new proton-conducting materials with improved performance(J. Chen et al., 2022). Although some scientists are trying to explore the proton transfer mechanism by using the MOFs represent an intriguing type of crystalline porous materials, it's still very challenging to insight into the proton transfer mechanism in crystalline porous materials and the mechanism of the proton conduction is indistinct because of the lack of crystallinity in MOFs (Zhang et al., 2021). Furthermore, the structures of most MOFs are unstable and liable to collapse under high temperature and high humidity conditions, which severely limits their application in devices. Therefore, developing a material with improved proton conductivity and structural stability is crucial for further application in CPs and MOFs(X. Chen & Li, 2020). Based on the above considerations, in this paper, with the introduction of organic ligands with functional groups, the proton conductivity of a stable Lead tartrate tetrahydrate structural model is improved where the acidity and hydrophilicity of the material are enhanced to form proton conducting pathways. Lead tartrate tetrahydrate has well-known highly structural and chemical stabilities, assembled with acid ligands that serve as proton hopping sites to meet the requirements of fuel cells, excellent proton conductivity, high fuel barrier performance, and stability.

2. LITERATURE SURVEY

(Saravanabharathi et al., 2019) obtained two crystalline forms differing in the number of lattice water molecules, depending on the duration of crystallization. X-ray structural studies were performed and additional water molecules in form II were confirmed using contact angle measurements. Procedures were optimized for better crystalline yields, and the bulk purity was ascertained by Thermogravimetric analysis (TGA), elemental and PXRD analysis. Alternate Current (AC) impedance measurements proved that both the crystalline forms were indeed proton-conducting electrolytes under humidified conditions at 25 ◦C.

(Zou et al., 2021) took a zirconium-based metal−organic framework (UiO-66), as a prototype, and functional post modification via the versatile Cu(I)-catalyzed azide−alkyne "click" reaction was carried out, and sulfonic acid groups were successfully grafted into its skeleton. Investigations by electrochemical impedance spectroscopy measurements revealed that its proton conductivity increases exponentially more than those of the existing organic frameworks, respectively, at the RH conditions. The high performance in long-life reusability of the resultant MOF demonstrated that the "click" reaction is robust porous materials toward targeted applications.

(Moi et al., 2020) incorporated both amine and sulfonates in anticipation of producing an alternate proton-conducting material called amine and sulfonates incorporated MOF (Cu-SAT) with superior proton conductivity. It exhibited high stability in water¸ stability to dilute hydrochloric acid as well as remarkable proton conductivity at 353 K and 98% RH. As a step ahead towards the practical application of the material in proton exchange membrane fuel cell (PEMFC)¸ the composite membranes of Cu-SAT and poly (vinylidene fluoride) (PVDF)-poly(vinylpyrrolidone) (PVP) matrix had further been fabricated, which displayed proton conductivity as high as at 353 K and 98% RH.

(X. M. Li et al., 2019) introduced a hierarchical modification strategy for the improvement of proton conductivity in a stable MOF model system. Initially, Zirconium aminobenzenedicarboxylate MOF (UiO66-NH_2) was synthesized. Then, the UiO-66-AS is obtained by the partial substitution of ligand 2-aminoterephthalic acid (BDC-NH2) with monosodium 2-sulfoterephthalate (BDC-SO_3Na). Results showed that there was an enhancement in proton conductivity with outstanding long-term stability.

(Shi et al., 2020) explored three hydrogen-bonded supramolecular frameworks (HSFs) and elaborated with success. With the adoption of imidazole multi-carboxylate ligand, the HSFs 1-3 showed high water and chemical stability. Meanwhile, the high proton conducting performance was achieved by the hydrogen bond networks inside the frameworks formed by imidazole unit, carboxylate groups, and crystallized water molecules. The report demonstrated promising application potentials of such crystalline materials in the electrochemistry field.

(Javed et al., 2020) prepared Large Co-MOF-74 crystals of a few hundred micrometers by solvothermal synthesis, and their structure and morphology were characterized. The hydrothermal stability of the material up to 60 °C at 93% relative humidity was verified by temperature-dependent XRD. Proton conductivity was studied by impedance spectroscopy using a single crystal. By varying the relative humidity (70–95%), temperature (21–60 °C), and orientation of the crystal relative to the electrical potential, it was found that proton conduction occurs predominantly through the linear and unidirectional (1D) micropore channels of Co-MOF-74.

(Wang et al., 2021) adopted the strategy of doping metal−organic frameworks (MOFs) with guest molecules into the Nafion matrix to improve the electrochemical performance of Nafion hybrid membranes. The high proton-conducting Zn-MOFs were used with the characteristics of host−guest collaborative hydrogen bonds as the filler to prepare Zn-MOF/Nafion hybrid membranes. AC impedance tests showed that when the doping amount of Zn-MOF was 5%, the proton conductivity reaches 1.87 times that of the pure Nafion membrane at 58% RH and 80 °C. This study provided a promising method for optimizing the structure of MOF proton conductors and inspires the preparation of high-performance Nafion hybrid membranes.

(Wang et al., 2020) prepared the coordination polymer $\{[Co_3L_2(H_2O)_6]\cdot 2H_2O\}n$ and the aqueous-phase Single Crystal to Single Crystal (SC-SC) central metal exchange product $\{[Cu_3L_2(H_2O)_6]\cdot 2H_2O\}n$. The daughter product presents a higher proton conductivity at 95 °C and 100% RH, increasing by 50-fold relative to the parent product. The water vapor adsorption revealed that the uptake capacity of 2 reaches 7.5 times higher than that of 1. Replacing water vapor with vapors of dilute hydrochloric acid and ammonia, the improvement of proton conductivity was also realized.

(R. Li et al., 2017) developed a highly anisotropic proton-conductive 2D MOF with definite crystal structures showing single-crystal to single-crystal transformation between the anhydrate (1) and trihydrate phases. The highest proton conductivity of $1\cdot 3H_2O$ at 80°C and 95% relative humidity was observed among the reported 2D MOF crystals. The relation between the proton conductivity and structure was also revealed. The time-dependent proton conductivity and single-crystal X-ray diffraction measurements demonstrated that $1\cdot 3H_2O$ was temperature and humidity-stable and acts as an underlying electrolyte material for fuel cell applications.

(Bunzen et al., 2019) presented a new proton-conducting iron (II) MOF of an unusual structure formed by chains of alternating bistriazolate-p-benzoquinone anions and iron (II) cations with four axially coordinated water molecules. Those chains are assembled via π-π stacking between the aromatic units

to form a three-dimensional grid-like network with channel pores filled with water molecules. The material was structurally characterized by single crystal XRD analysis, and its water and thermal stability were investigated. The proton conductivity was studied by impedance measurements on needle-like single crystals. The iron(II)-MOF showed the highest proton conductivity at 22 °C and 94 % relative humidity.

(Yang et al., 2017) reported a chemically stable and structurally flexible MOF, BUT-8(Cr)A, possessing a three-dimensional framework structure with one-dimensional channels, in which high-density sulfonic acid ($–SO_3H$) sites are arranged on channel surfaces for proton conduction. Also, presented that its flexible nature, together with its $–SO_3H$ sites allowed BUT-8(Cr)A to self-adapt its framework under different humid environments to ensure smooth proton conduction pathways mediated by water molecules. Relative to other MOFs, BUT-8(Cr)A not only had a high proton conductivity at 100% RH and 80 °C but also maintains moderately high proton conductivity at a wide range of RH and temperature.

(Wahiduzzaman et al., 2019) prepared titanium carboxylate-based MOF, incorporating hydrogen-sulfate functions bounded to Ti-metal sites using a green and simple synthesis protocol. This solid exhibited very high proton conductivity at 298 K and 95% relative humidity as evidenced by impedance spectroscopy measurements. This high level of performance maintained over 7 days combined with very good chemical stability and green synthesis route positions showed that MOF is a promising candidate for further deployment as a proton-exchange membrane.

(Wei et al., 2017) synthesized three nonporous coordination compounds with the HCl steaming-assisted conversion approach by using a multi-functional group, including the sulfonate group and the Clorine (Cl)- or Hydrogen Phospate (HPO_4^{2-}) group. The protonated sulfonate group together with the halide Cl- group played a positive role in increasing proton conductivity; meanwhile, the packing mode of the structure was also an important factor influencing proton conduction. The compounds exhibited high proton conductivity values at 95 °C and 97% RH; in this, compound 2 exhibited the highest value at 97% RH and 368K.

(Rao et al., 2017) constructed a well-interconnected MOF structure (GO@UiO-66-NH2)by tethering the effect of Graphine Oxide (GO) surfaces and interconnection among MOF grains. It was found the synergistic effect between GO and UiO-66-NH_2 with suitable particle size was especially important for promoting proton transfer. Such interconnected structures of MOF on GO also made acid/base pair pathways between Sulphonic Acid ($–SO_3H$) of Nafion and Amino Group ($–NH_2$) of GO@UiO-66-NH_2 more consecutive. That was favorable to proton conduction via both the vehicle mechanism and the Grotthuss mechanism. The proton conductivity of the as-prepared composite membrane reached maximum conductivity under 90 °C and 95% RH, respectively.

(Xing et al., 2019) synthesized a new Gadolinium (III) (Gd(III)) MOF, $\{H[(N(CH3)_4)_2][Gd_3(NIPA)_6]\}3H_2O$. The new MOF with excellent water stability, $\{H[(N(CH3)_4)_2][Gd_3(NIPA)_6]\}3H_2O$ displayed an optimal proton conductivity at 75°Cand 98% relative humidity, which was among the highest values for proton-conducting MOFs. The results demonstrated that it possessed high moisture sensitivity and formed more hydrogen-bonded networks at high RH.

3. EXPERIMENTAL DESIGN

An experimental design is the list of steps taken and the order to do the experiment. Experimental design is divided into two sections, in which, the first section details the specific

techniques used for conducting the experiment, and the experimental execution of the taken material is given in the next section.

3.1 Measurements and Characterization

The FTIR spectral analysis of the powdered and pelletized sample was recorded ranging from 400– 4500 cm^{-1}. In order to record the FTIR spectrum, a KBr pellet technique was used, wherein, the Lead tartrate sample was thoroughly grounded with solid KBr. The resulting solid mixture was compressed by giving an appropriate pressure to form a thin transparent pellet. The FTIR measurements of the sample were recorded using Shimadzu 8400S FT-IR spectrophotometer as KBr pellet under different conditions. PXRD patterns were collected in the 2θ range on a Shimadzu Lab Model 6000 XRD instrument. The conductivity measurements are carried out for the materials using pellets of 1.3 (cm) diameters and 0.18 cm thickness at a pressure of 100 $kg\,cm^{-2}$. The opposite sides of the pellets were coated with silver paint and inserted between two conducting surfaces with a screw load to ensure better electrical contact. In order to ensure moisture saturation, the sample was kept in a closed chamber with distilled water allowing to stand for 24 hrs. The electrical conductivity is measured in the temperature range 35-55°C at 5°C intervals using the two probe impedance analyzer in Gamry 600 Potentiostat/Galvanostat/FRA over a frequency range of 1MHz-10MHz. The two-probe technique consists of contacting two probes or contacts on the specimen and measuring the voltage while a current is applied between the probes. The conductivity of the sample was calculated using,

$$\sigma_{con} = \frac{T}{\mathrm{Im} \times EA} \tag{1}$$

Where, σ_{con} is the conductivity $(S\,cm^{-1})$, T is the sample thickness (cm), Im is the impedance value, and EA is the electrode area (cm^2) of the sample, respectively. The value of impedance used for this calculation is the resistance estimated from the intersection (at high-frequency) of the real axis (Z') and the semicircle of the nyquist plot.

3.2 Preparation of the Complex

The crystal structure of Lead L-tartrate tetrahydrate has been prompted by the coordination of metal atoms with carboxylic acids. In this work, the Lead(II) metal ion is coordinated with the Sodium Potassium tartrate acid. Single crystals of $PbC_4H_4O_6{\cdot}4H_2O$ were obtained by slow evaporation of an aqueous solution of L tartaric acid and Lead Nitrate at room temperature. Lead Nitrate ($Pb(NO_3)_2$) and Sodium Potassium tartrate ($C_4H_4O_6KNa{\cdot}4H_2O$) were separately prepared and dissolved separately in water to get a saturated solution. Potassium sodium L-tartrate is the organic sodium and potassium salt of L-tartaric acid. In the synthesis of Lead Tartrate, 1.5 g of dextro-tartaric acid was dissolved in 100 ml of water and was handled with 500 g of solid sodium bi-carbonate and 200-g of potassium bicarbonate. Then, the saturated solutions are added to the complete mixing of the reactants. After that, the mixture is boiled and filtered. The resulting solution is kept undisturbed for two days. During this process, the formation of crystals was noticed and quality crystals were obtained within a few hours. Colorless crystals of Lead tartrate separated out from the solution. The crystals were separated from the solution and used for electrochemical studies.

4. RESULTS AND DISCUSSION

The crystals of $PbC_4H_4O_6{\cdot}4H_2O$ were characterized by FT-IR spectroscopy. This section contains the experimental results through the FT-IR, PXRD, and Proton conductivity measurements. The measurement was performed under 100% relative humidity (RH).

4.1 Synthesis and Structural Features

This section analyses the structural features to evaluate the quality of the present method of crystallization, which involves only a simple mixing of the aqueous solutions as an additive at room temperature. This offers a different approach for designing and fabricating proton-conducting materials and enables the construction of proton conduction channels with diverse surfaces. Thus, the mixing procedure is depicted in figure 1,

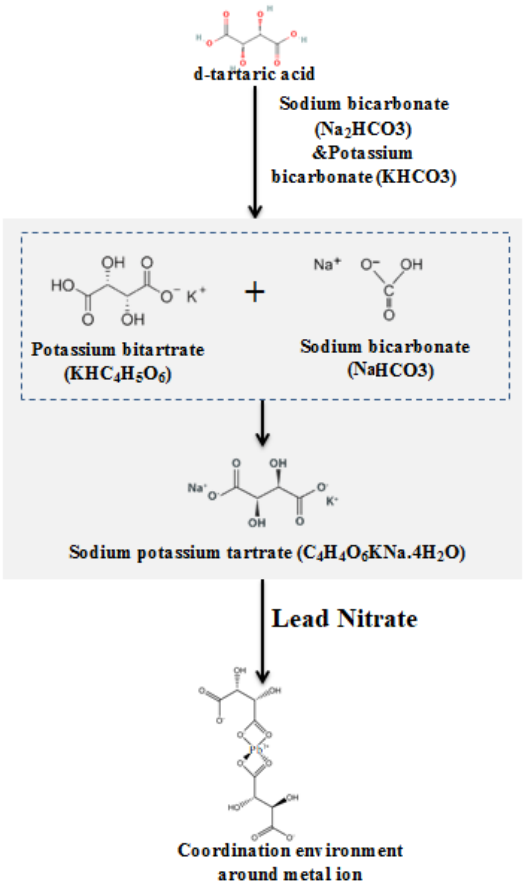

Figure 1: Preparation of presented proton conducting material

This process establishes an efficient way for the present model to produce crystalline products of quantitative yield within a few hours. It was observed that, while mixing, fine single crystals quickly settled down at the bottom of the vessel for the separation of crystalline products from the parent liquor. Hence, the crystallization of Lead tartrate using the Rochelle salt and Lead Nitrate solutions appears to be very simple and convenient in contrast to that of the previous methods. Also, the results signify that the present method reduces the time and effort of crystallization, by yielding the compound directly in a single lot. The Lead atom is six-coordinated four from two chelate rings of two tartrate ions, and two water molecules and the average distance from the lead atom to the four nearest neighbours is about 2.514 Å, which can be best described as slightly distorted. Each of these water molecules is bonded to the oxygen atoms of the adjacent tartrate groups by hydrogen bonds. Most interchain linkage is provided by the network of hydrogen bonds formed by the additional water molecules. The structural reports show the presence of two more lattice water molecules, thus forming the molecular formula to be $PbC_4H_4O_6 \cdot 4H_2O$.

4.2 FT-IR Analysis

In order to evaluate the synthesized material, FTIR spectroscopy, which can often serve as the material analysis process is established. FTIR offers quantitative and qualitative analysis for organic and inorganic samples. Fourier Transform Infrared Spectroscopy (FTIR) identifies chemical bonds in a molecule by producing an infrared absorption spectrum. The spectra produce a profile of the sample and a distinctive molecular fingerprint that can be used to screen and scan samples for many different components. The FT-IR offers the spectra of other metal–tartrate complexes that support the solid-state structural features of the sample. In order to analyze the structural integrity of the system, it is necessary to learn the appearance peaks through spectroscopic methods under relevant conditions. In this regard, the solidity of the sample has been studied using the FT-IR experimentsafter exposure to moisture and after drying in a Desiccator. The spectrum is recorded on a graph with wave number (cm^{-1}) recorded on the X-axis and transmittance recorded on the Y-axis.

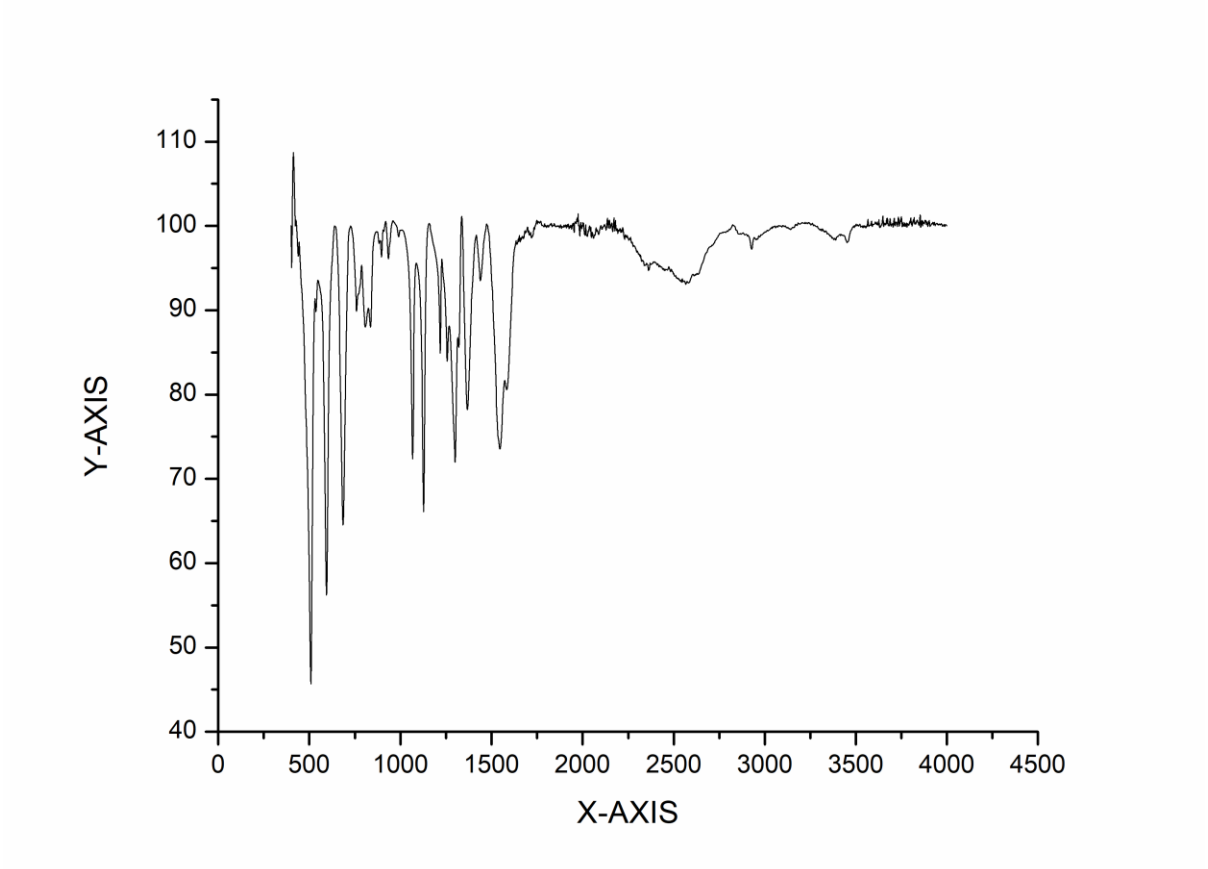

(a)

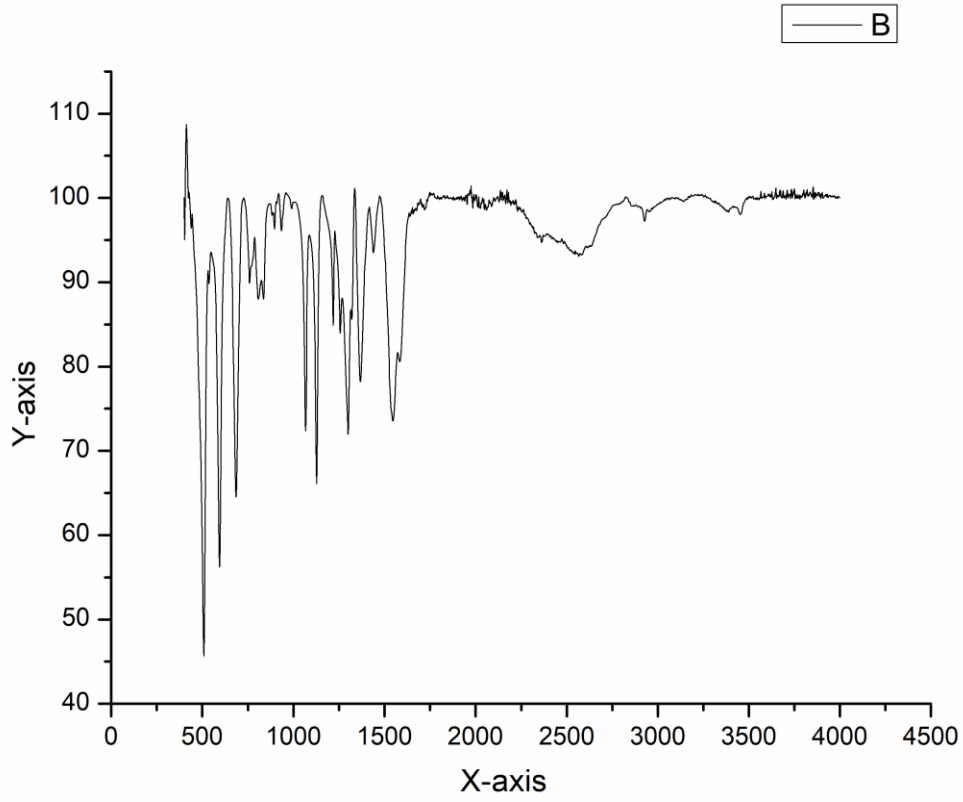
B
Y-axis
X-axis
110
100
90
80
70
60
50
40
0
500
1000
1500
2000
2500
3000
3500
4000
4500

(b)

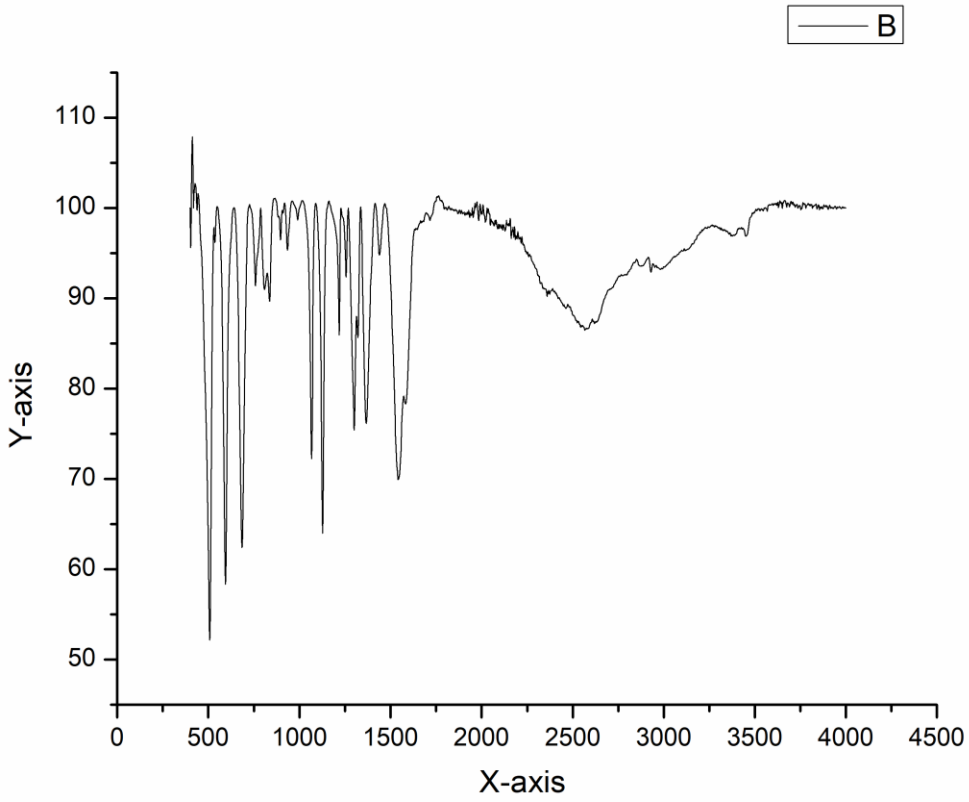
B
Y-axis
X-axis
110
100
90
80
70
60
50
0
500
1000
1500
2000
2500
3000
3500
4000
4500

(c)

Figure 2: The similarity of IR spectra of the manufactured sample with respect to various conditions **(a)** as synthesized**, (b)** after dried in a dessicator, and **(c)** exposing the dried phase to moisture

In the above figure 2, the huge absorptions observed close to 1580 (cm^{-1}) and 1670 (cm^{-1}) that are corresponding to the vibrations of the carbonyl C=O group of the tartrate ligands and inform the existence of active carbonyl groups. The broad O−H stretching region between 2985 (cm^{-1}) and 3957 (cm^{-1}) confirms the existence of several types of water molecules interacting through Hydrogen bonds with variable strength. Thus, this indicates the presence of water in crystallization. Also, no significant difference was observed in hydroxyl functionalities for the three conditions. Figure 2 exhibit a medium band between 1481 (cm^{-1}) and 1231 (cm^{-1}) which is attributed to the C-O stretching vibrations. The band in the region of 1143 (cm^{-1}) to 1049 (cm^{-1}) is attributed to the out-of-plane O-H deformation and C-O stretching of the alcoholic groups. The band below 928 (cm^{-1}) indicates the presence of calcium–oxygen stretching vibrations. Based on the analysis, the presence of the O-H, C-O, C=O, water of hydration, and calcium-oxygen bonds are established from the spectra. The outcome reveals that the freshly prepared material has good agreement with the chemical compound, and proves the robustness of the system in all conditions.

4.3 PXRD Analysis

PXRD traces are also useful in examining the stabilities of the compound under various common environmental conditions in relevance to the proton conductivity studies. Hence, in the present study, to gauge the stability and materialistic worthiness of the crystalline forms, Thermo Gravimetric Analyses (TGAs) were performed on a bulk sample with a powder X-ray diffraction (PXRD) pattern matching crystal data. The x-axis shows that the pattern is measured in 2θ and the y-axis is the relative intensity of the diffracted beam. In this case, the width of the peak would reveal the average crystalline size of a nanoparticle where sharp peaks indicate a large size of crystallites, whereas broad peaks indicate smaller crystallites.

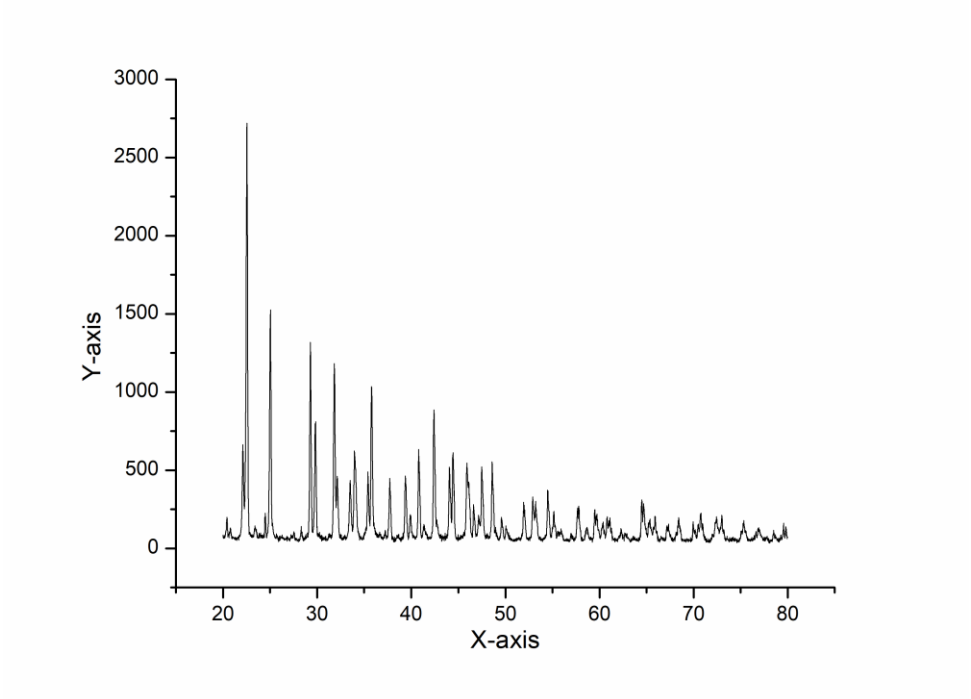

(a)

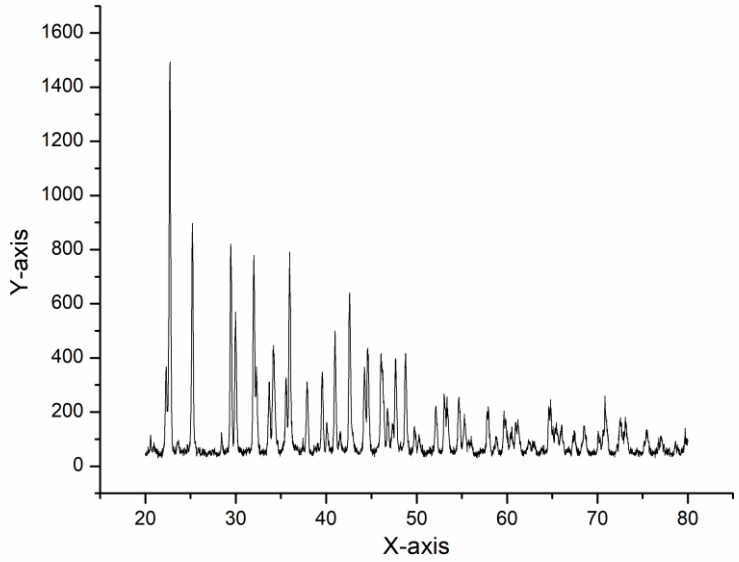

(b)

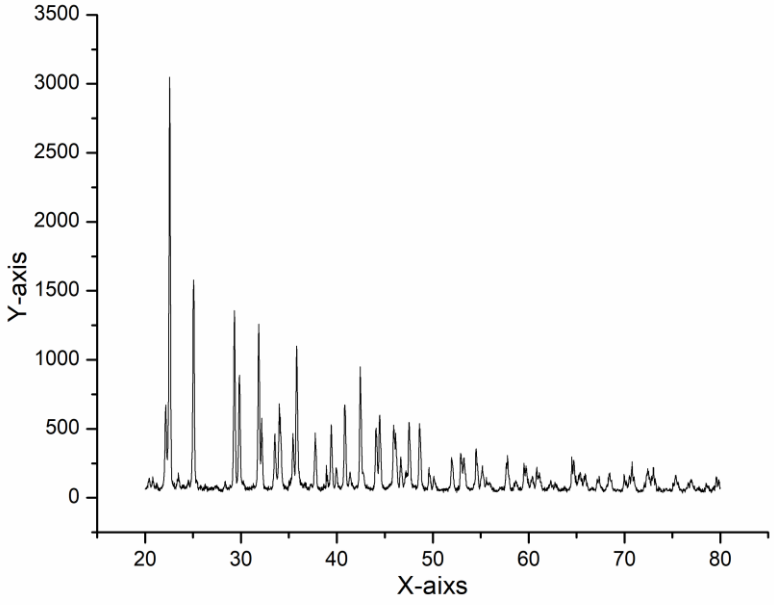

(c)

Figure 3: PXRD patterns of the sample recorded under **(a)** as synthesized, **(b)** after dried in a desiccator and **(c)** exposing the dried phase to moisture conditions

The PXRD patterns recorded at the run of 100% relative humidity conditions and 2θpositions are shown in the figure 3. To ascertain the type and quantity of the crystalline phase of the material, the experiments have been performed by exposing the samples to moisture and drying them in a

Desiccator, and matching them with those of the as-synthesized pattern in their respective 2-theta positions. For all cases, the as-synthesized bulk materials confirm the phase purity with identical emergence of peak positions with their corresponding simulated patterns. The greater the intensity of the peak the greater will be the number of crystals or molecules with that distinct spacing. When the crystallite size decreases from bulk to nanoscale dimensions, the XRD peaks broaden. The pattern of the sample under moisture environments in figure 3(b) matches very closely with that of the Figure 3(a). The peaks observed for the PXRD outcome of the dried phase in figure 3(c) largely resemble the pattern of Figure 3(a). in their respective 2θ positions. When compared to the calculated patterns in Figure 3(a), the peak positions indicate that they are possibly attributed to factors, such as reduction in particle size by filling of humidity into the pores during sample preparations and also at the time of X-ray diffraction. The sharp and well-defined PXRD profile of the compound matching with those of the simulated profile derived from the single crystal structure solution illustrates that the samples are indeed stable under such environments and hence they are reliable for impedance measurements. Remarkably, the corresponding PXRD patterns of all the materials were identical to that of the parent material proving that the materials had excellent stability, which is essential for their practical application in fuel cells.

4.4 Proton Conductivity Studies

There are certain structural features that make good candidates as proton-conductors that have the possibility of proton conductivity behaviour at room temperature. Therefore, conductivity studies have been carried out for one representative member of each series. The Nyquist plots were recorded for the powdered and pelletized Lead tartrate sample, with time. To examine the proton conductivity of the sample Alternating Current (AC) impedance was first carried out. Impedance spectra were recorded by exposing the pellet to 95% humidity atmosphere; the spectra were recorded by superimposing an AC sinusoidal voltage of 50 mV at the open circuit potential in the frequency range 1.0 MHz to 10 mHz. Impedance spectra for the Manganesetartrate sample at different relative humidity values and temperatures were collected, and the impedance data were used to draw Nyquist plots that are represented in a complex impedance plane consisting of real impedance (Z') in X-axis and imaginary impedance (Z'') in Y-axis. The evaluation of Nyquist plots is shown in Figures 4 and 5, respectively,

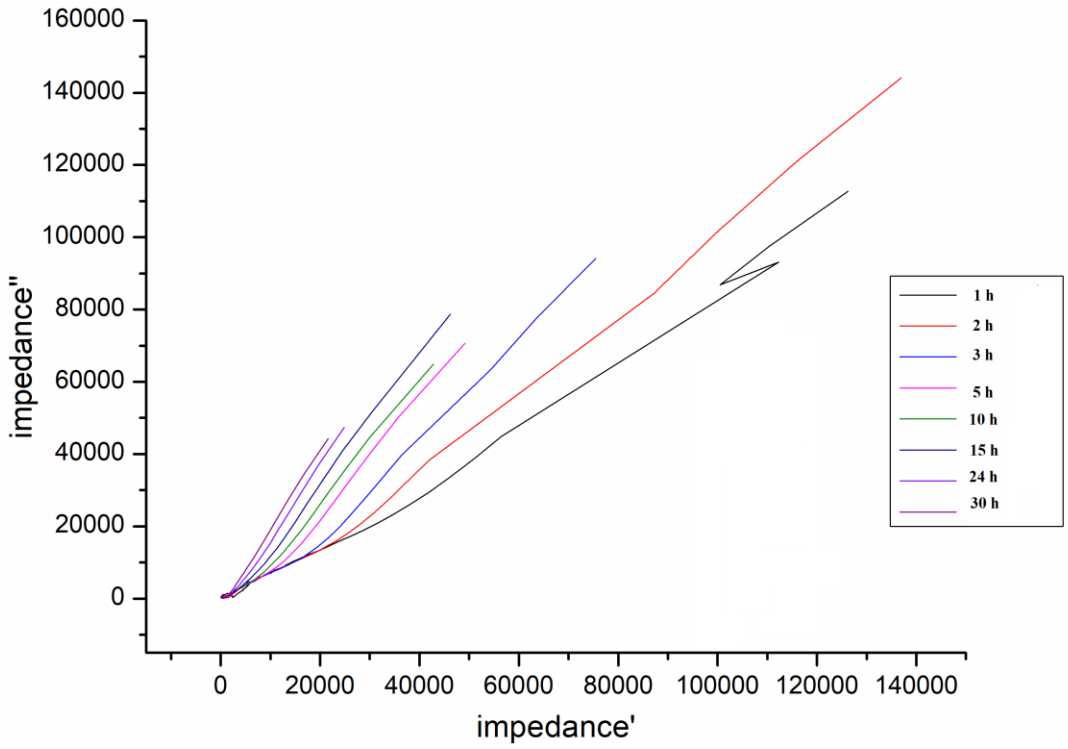

Figure 4: Impedance spectra of the sample by exposing the pellet to 95% humidity from **1 h to 30 h**

In the experiments, the sample was dried in a desiccator and the impedance spectra were recorded to check the reproducibility. It was expected that the Nyquist plots become a depressed semicircle representing the internal impedance of the material. Figure 4 shows the time-dependent measurement of the Lead tartrate at 25 °C and 98% RH. So, this variation of conductivity with time is typical of the materials that are showing ionic conductivity in between the ion-blocking electrodes. Proton conductivity is one of the key parameters in determining the performance of proton exchange membranes. The transport mechanism within the membrane is attributed to the protons hopping through the network of hydrogen bonds and protons bound to the acid molecule moving through the membrane. The porous nature significantly increases the Lewis acidity of the water molecules that are coordinated with the metal centers and improves proton conductivity. From Figure 4, it can be stated that the sample with longer treatment times exhibited excellent proton conductivities. When the sample is treated for 1 h min to 30 h, the charge transfer resistance attained by the sample varies as, 30904.36, 16061.61, 6636.53, and 4167.34. Consequently, for the extension of time from 70 min to 100 min also the resistance achieved is, 8639.52, 2836.24, 2506.43, and 2205.38. It was also found that the charge transfer resistance decreases with respect to the extension of time, and further it represents the major participation to the improved proton conductivity of the sample. The proton conductivity of the sample at the end of 60 min reaches $4.5\times10^{-5}\,S\,cm^{-1}$ and $8.4\times10^{-4}\,S\,cm^{-1}$ after being treated for 100 mins. As a result, the material shows a high proton conductivity of $8.4\times10^{-4}\,S\,cm^{-1}$, measured at a relative humidity (RH) of 98% and 25 °C. The high proton conductivity was attributed to the internal H-bonding networks. It was found that the sample retained high proton conductivity even after 100 mins, and the loss of conductivity was negligible. The presence of water content with increased RH obviously enhances the proton conductivities, which implies that protons primarily migrate through the inner pores of the presented model. These

observations clearly suggest the fact that the presence of moisture is very crucial in establishing the conductivity characteristics in both systems and therefore it could be realized that the protons are the charge carriers during the conduction processes.

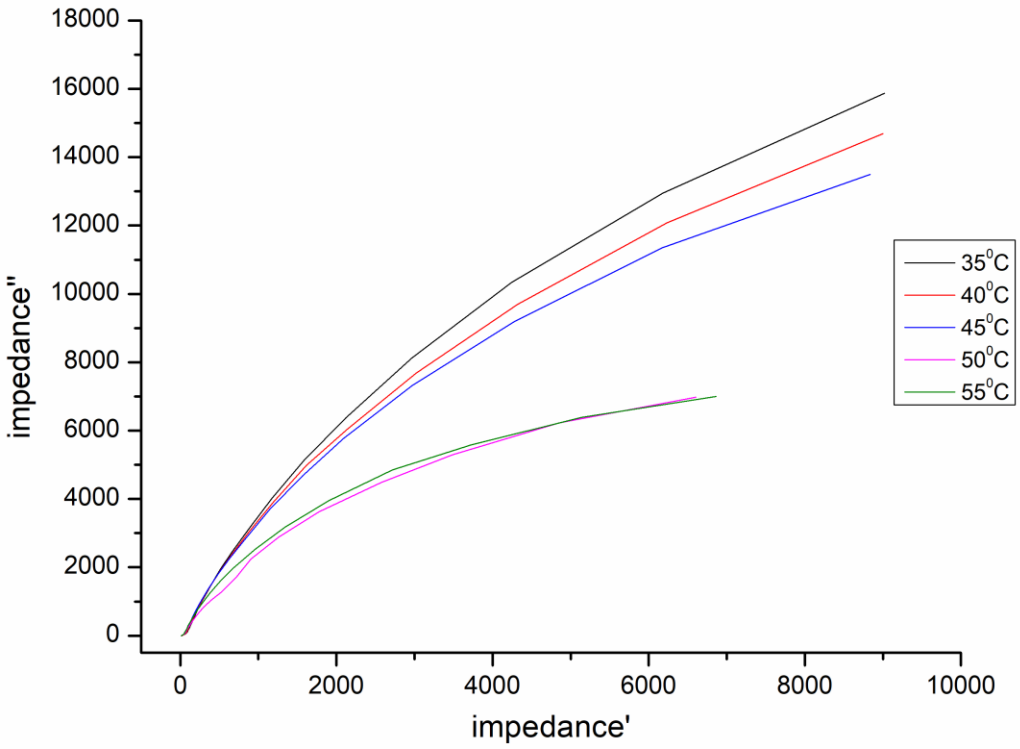

Figure 5: Temperature dependent Nyquist plot at 35 °C to 55 °C

The conductivity measurement under temperature sweeping from 35°C to 55°C is shown in above figure 5. The effect of temperature on the proton conductivity was studied using Impedance spectroscopy. The straight lines with large slopes at lower temperatures indicate the insulating behaviour of the material. However, on increasing temperature, the slope of the lines decreases, and hence they bend towards the Z′ - axis by which a semicircle could be formed. The characteristic Nyquist plots indicate that the sample exhibit protonconductivity increases with an increase in temperature. As shown in Figure 5, the charge transfer resistance is calculated as 651.917 at 35 °C and 98% RH, while the values are only 442.28 and 333.86 at 45 °C and 50 °C, respectively, at the same condition. The reduction in charge transfer resistance indicates an increase in proton conductivity. It is clear from figure 5 that the extensive hydrogen-bonding network in the crystal lattice leading to high, temperature- and humidity-dependent proton conductivities.

5. CONCLUSION

Proton conductivity is an important property of proton-conducting materials, which can directly affect the fuel cell's performance. In this paper, an environmentally benign coordination

polymer called Lead L-tartrate tetrahydrate is successfully implemented as a solid electrolyte and achieved extremely high proton conductivity. In summary, here a modified strategy for the crystallization phase of the compound is presented and the structural stability of the model is improved with the entry of proton sources. Furthermore, the proton conductivity studies demonstrate its good durability and stability. The increased proton conductivity at 25 °C and 98% RH is comparable to the reported proton-conducting MOF material and also showed outstanding water stability with a negligible conducting loss even after continuously working for longer duration. The proton conductivity is strongly humidity-dependent. These findings indicate that water molecules in the channels provide a proton-conducting path and the material can be considered as the most stable proton conductor based on a MOF with high proton conductivity.

REFERENCES

Biradha, K., Goswami, A., Moi, R. and Saha, S., 2021. Metal–organic frameworks as proton conductors: strategies for improved proton conductivity. *Dalton Transactions*, *50*(31), pp.10655-10673.

Bunzen, H., Javed, A., Klawinski, D., Lamp, A., Grzywa, M., Kalytta-Mewes, A., Tiemann, M., von Nidda, H.A.K., Wagner, T. and Volkmer, D., 2018. Anisotropic water-mediated proton conductivity in large iron (II) metal–organic framework single crystals for proton-exchange membrane fuel cells. *ACS Applied Nano Materials*, *2*(1), pp.291-298.

Chen, J., Mei, Q., Chen, Y., Marsh, C., An, B., Han, X., Silverwood, I.P., Li, M., Cheng, Y., He, M. and Chen, X., 2022. Highly Efficient Proton Conduction in the Metal–Organic Framework Material MFM-300 (Cr)· SO4 (H3O) 2. *Journal of the American Chemical Society*, *144*(27), pp.11969-11974.

Chen, X. and Li, G., 2020. Proton conductive Zr-based MOFs. *Inorganic Chemistry Frontiers*, *7*(19), pp.3765-3784.

Guccini, V., Carlson, A., Yu, S., Lindbergh, G., Lindström, R.W. and Salazar-Alvarez, G., 2019. Highly proton conductive membranes based on carboxylated cellulose nanofibres and their performance in proton exchange membrane fuel cells. *Journal of Materials Chemistry A*, *7*(43), pp.25032-25039.

Javed, A., Strauss, I., Bunzen, H., Caro, J. and Tiemann, M., 2020. Humidity-mediated anisotropic proton conductivity through the 1D channels of Co-MOF-74. *Nanomaterials*, *10*(7), p.1263.

Kolokolov, D.I., Lim, D.W. and Kitagawa, H., 2020. Characterization of Proton Dynamics for the Understanding of Conduction Mechanism in Proton Conductive Metal- Organic Frameworks. *The Chemical Record*, *20*(11), pp.1297-1313.

Lee, J.S.M., Otake, K.I. and Kitagawa, S., 2020. Transport properties in porous coordination polymers. *Coordination Chemistry Reviews*, *421*, p.213447.

Li, R., Wang, S.H., Chen, X.X., Lu, J., Fu, Z.H., Li, Y., Xu, G., Zheng, F.K. and Guo, G.C., 2017. Highly anisotropic and water molecule-dependent proton conductivity in a 2D homochiral copper (II) metal–organic framework. *Chemistry of Materials*, *29*(5), pp.2321-2331.

Li, T., Zhang, L.X., Xing, Y., Xu, H., Yue, Y.Q., Li, Q., Dong, H., Wang, H.Y. and Yin, Y.Y., 2019. A ciprofloxacin based 1D Cd (II) coordination polymer with highly efficient humidity sensing performance. *Inorganic Chemistry Communications*, *108*, p.107541.

Li, X.M., Liu, J., Zhao, C., Zhou, J.L., Zhao, L., Li, S.L. and Lan, Y.Q., 2019. Strategic hierarchical improvement of superprotonic conductivity in a stable metal–organic framework system. *Journal of Materials Chemistry A*, *7*(43), pp.25165-25171.

Lim, D.W. and Kitagawa, H., 2021. Rational strategies for proton-conductive metal–organic frameworks. *Chemical Society Reviews*, *50*(11), pp.6349-6368.

Moi, R., Ghorai, A., Banerjee, S. and Biradha, K., 2020. Amino-and sulfonate-functionalized metal–organic framework for fabrication of proton exchange membranes with improved proton conductivity. *Crystal Growth & Design*, *20*(8), pp.5557-5563.

Rao, Z., Feng, K., Tang, B. and Wu, P., 2017. Construction of well interconnected metal-organic framework structure for effectively promoting proton conductivity of proton exchange membrane. *Journal of Membrane Science*, *533*, pp.160-170.

Saravanabharathi, D., Obulichetty, M. and Kumaravel, M., 2019. Facile crystallization of 2-phenyl benzimidazole-5-sulfonic acid: Characterization of lattice water dependent zwitterionic supramolecular forms, with modulation in proton conductivities. *Journal of Chemical Sciences*, *131*, pp.1-13.

Sazali, N., Wan Salleh, W.N., Jamaludin, A.S. and Mhd Razali, M.N., 2020. New perspectives on fuel cell technology: A brief review. *Membranes*, *10*(5), p.99.

Shi, Z.Q., Ji, N.N., Guo, K.M. and Li, G., 2020. Crystalline hydrogen-bonded supramolecular frameworks (HSFs) as new class of proton conductive materials. *Applied Surface Science*, *504*, p.144484.

Wahiduzzaman, M., Wang, S., Schnee, J., Vimont, A., Ortiz, V., Yot, P.G., Retoux, R., Daturi, M., Lee, J.S., Chang, J.S. and Serre, C., 2019. A high proton conductive hydrogen-sulfate decorated titanium carboxylate Metal− Organic framework. *ACS Sustainable Chemistry & Engineering*, *7*(6), pp.5776-5783.

Wang, H., Wu, Q., Ding, X., Shao, Z., Xu, W., Zhao, Y., Xie, Q., Meng, X. and Hou, H., 2020. The 50-fold enhanced proton conductivity brought by aqueous-phase single-crystal-to-single-crystal central metal exchange. *Inorganic Chemistry*, *59*(12), pp.8361-8368.

Wang, H., Zhao, Y., Shao, Z., Xu, W., Wu, Q., Ding, X. and Hou, H., 2021. Proton Conduction of Nafion Hybrid Membranes Promoted by NH3-Modified Zn-MOF with Host–Guest Collaborative Hydrogen Bonds for H2/O2 Fuel Cell Applications. *ACS Applied Materials & Interfaces*, *13*(6), pp.7485-7497.

Wei, M.J., Fu, J.Q., Wang, Y.D., Zhang, Y., Zang, H.Y., Shao, K.Z., Li, Y.G. and Su, Z.M., 2017. Highly tuneable proton-conducting coordination polymers derived from a sulfonate-based ligand. *CrystEngComm*, *19*(46), pp.7050-7056.

Xing, X.S., Fu, Z.H., Zhang, N.N., Yu, X.Q., Wang, M.S. and Guo, G.C., 2019. High proton conduction in an excellent water-stable gadolinium metal–organic framework. *Chemical communications*, *55*(9), pp.1241-1244.

Bobkov, Y.V., Walker III, W.B. and Cattaneo, A.M., 2021. Altered functional properties of the codling moth Orco mutagenized in the intracellular loop-3. *Scientific Reports*, *11*(1), pp.1-16.

Zhang, G., Jin, L., Zhang, R., Bai, Y., Zhu, R. and Pang, H., 2021. Recent advances in the development of electronically and ionically conductive metal-organic frameworks. *Coordination Chemistry Reviews*, *439*, p.213915.

Zou, X.N., Zhang, D., Xie, Y., Luan, T.X., Li, W., Li, L. and Li, P.Z., 2021. High Enhancement in Proton Conductivity by Incorporating Sulfonic Acids into a Zirconium-Based Metal–Organic Framework via "Click" Reaction. *Inorganic Chemistry*, *60*(14), pp.10089-10094.